EFFECT OF GRAIN BOUNDARY MISORIENTATION ON THE ASYMMETRY, ANISOTROPY, AND NUCLEATION STRESSES OF $\{10\bar{1}2\}$ TWINNING AND NON-BASAL SLIP IN MAGNESIUM

J.C. Baird[2], H. El Kadiri[1,2], A.L. Oppedal[2], J. Kapil[2], Q. Ma[2], M.F. Horstemeyer[1,2], S. C. Vogel[3]

Department of Mechanical Engineering, Mississippi State University, MS 39762, USA
Center for Advanced Vehicular Systems, Mississippi State University, MS 39762, USA
Los Alamos Neutron Science Center, Los Alamos National Laboratory, NM, 87545, USA

Keywords: Twinning stress, Magnesium, Crystal Plasticity, Grain Boundary Misorientation

Abstract

Early reports pertaining to Non-Schmid phenomena of both slip and twinning in BCC and HCP structures and their effect on anisotropy and asymmetry were essentially attributed to either unusual activities of screw dislocations or to a certain solute effects on dislocation activity. In this study, we show an important asymmetry of the $\{10\bar{1}2\}$ twinning and non-basal slip stresses that depend on the initial texture. Crystal plasticity simulations and non-destructive EBSD suggested that these non-Schmid effects correlate with the effect of mantle plasticity, which changed with the nature of initial texture. The critical stresses for both of these deformation mechanisms were identified to change by at least a factor of two for different initial textures of the same material composition. Sharp $[0002]$ fibers were revealed to cause softening of twinning and hardening of non-basal slip while axisymmetric textures hardened twinning and softened non-basal slip. While both non-basal slip and twinning correspond to extended and liberated partial dislocations, respectively, these reversed tendencies could not be explained unless slip and twinning are considered as mutually competitive mechanisms. As low misoriented grain boundaries harden slip, twinning becomes softer. Conventional crystal plasticity based on a pseudo-slip approach for twinning was unable to capture these mantle-induced textural effects related to the magnesium asymmetry.

Introduction

Despite intensive works during the 1950's, the fundamentals of twin nucleation are still a difficult challenge to many researchers dealing with the behavior of hexagonal-close packed (HCP) structures. The single crystal tests performed to verify whether or not twinning can be considered as a type of pseudo-slip deformation mechanism showed a surprising scatter in the critical resolved shear stress (CRSS)[1–11]. In general, the twinning stress exhibited a puzzling dependence on the microstructure, strain rate, temperature, stress state, prior slip, and texture. Fundamental studies on the generation of highly glissile twinning dislocations and their crystallography have since then been undertaken in an effort to develop physics-based models suitable for higher scale simulations such as crystal plasticity.

Recent literature has pointed to non-Schmid effects due to special cases of backstress, not arising from Geometrically Necessary Dislocations (GNDs), but arising from the incompatibility restrictions at the grain boundary segments where the residual twin lamella impinges [12–15]. These phenomena, however, relate to the forty-year old observations [16–21] on what researchers called accommodation effects and twin-twin interactions. Twin accommodation effects are in fact nothing else but a special case of backstress induced at the grain boundary (GB)/twin intersections, which give rise to either slip, twinning, or a crack so the twin can practically achieve its plastic deformation.

The influence of GBM on the twinning stress is a significant non-Schmid effect, because the pseudo-slip CRSS of twinning can change by varying the initial texture of the material, which actually predefines the GBM texture. In this paper, we further investigate these non-Schmid effects

by studying their effect on anisotropy and asymmetry of magnesium and exploring the capabilities of crystal plasticity to render the behavior of different textures obtained from the same material. In fact, crystal plasticity should, in principal, be texture-insensitive as long as the initial microstructure and composition remain largely unchanged. We use two types of texture: 1) a strongly concentrated ET $[0002]$ fiber texture (basal texture), and 2) a strongly sharp axisymmetric ED $\langle 10\bar{1}0 \rangle$ texture (rod-texture). Furthermore, because twinning and slip are competitive mechanisms, the GBM should not have a discriminatory influence on only twinning but on slip as well. The sensitivity of non-basal slip to GBM in HCP structures has not been investigated yet, and thus constitutes another important motivation of this paper. The results of mechanical testing and crystal plasticity simulations are substantiated by non-destructive electron backscattered diffraction (EBSD).

Experimental and simulation procedures

AM30 Mg samples were prepared in two different ways to generate two strong textures: (i) ED $\langle 10\bar{1}0 \rangle$ axisymmetric rod texture, and (ii) a ET $\parallel [0002]$ fiber texture. The rod texture was generated by extruding at approximately 530 °C of a 450 mm large cylindrical billet down to a billet of 180 mm diameter. This rod texture corresponded to a uniform distribution of the [0001] axis normal to the extrusion direction (ED). The basal texture was created using the same alloy composition but by extruding the 180 mm billet into 3 mm thick sheets (plane-strain extrusion). To keep the same final grain microstructure, the processing parameters were the same for both types of extrusions and were identified during the axisymmetric extrusion from billet to billet. A homogeneous axisymmetric texture allows the Schmid factor for {10-12} twinning to be uniformly constrained between 0.37 and 0.49 for nearly all grains under the ED compression. Both Neutron Diffraction (ND) and EBSD techniques were used to analyze the macrotexture and microtexture, respectively. All mechanical tests were performed at room temperature at a 0.001 s^{-1} strain rate. All samples were extracted through electrical discharge machining (EDM) in the form of 10 mm diameter cylinders. For non-destructive EBSD analyses, it was necessary for samples to have flat sections and were in form of cubes of 6 mm. Although many regions were analyzed by non-destructive EBSD at a strain increment of 0.05%, we only report typical results.

Figure 1 shows the initial texture of the two sample materials. Neutron diffraction texture analysis was done on the HIPPO neutron time-of-flight diffractometer at LANSCE [22]. The pole figure data was exported from MAUD [23] and imported into MTEX [24] for further Orientation Distribution analysis visualization.

This work uses the dislocation-density based hardening model developed by Beyerlein and Tomé [25] (based on equations of Kocks and Mecking [26,27]), and implemented into the Visco-Plastic Self-Consistent (VPSC) crystal plasticity model of the VPSC code [28]. For all simulations, five deformation modes were selected in the simulations:

(0001) $\langle \bar{2}110 \rangle$ (basal $\langle a \rangle$ slip), $\{10\bar{1}0\}\langle \bar{2}110 \rangle$ Prismatic $\langle a \rangle$ slip), $\{11\bar{2}2\}\langle 11\bar{2}3 \rangle$ (second order pyramidal $\langle c+a \rangle$ slip),

$\{1012\}\langle 1011 \rangle$ tension twins, and $\{10\bar{1}1\}\langle 10\bar{1}2 \rangle$ compression twins. More details on the model and fitting methodology of the simulations were described in a different paper [29,30].

Results and Discussion

Figure 2 shows the experimental and simulated stress-strain curves upon compression of the rod texture along the ED and ET. The parameters of the best fits were reported in a different paper [31], but the relative activities of deformation modes under ED (profuse twinning) are shown in Figure 3. This remarkable fit was particularly achieved owing to the dislocation transmutation concept incorporated in the model. The reckoning of dislocation transmutation for this material correlated with a twin which hardened three times more than the parent. Moreover, although ET

compression was dominated by slip, twinning was noticeable and reached approximately 40% of that upon ED (Figures 3). Nonetheless, the model captured well the stress-strain behavior under ET which illustrates, again, its robustness. To the author's knowledge, previous correlated models for magnesium were only shown to capture anisotropy in the two limiting cases of maximum twinning or no twinning. This topic is beyond the scope of this paper, but it is the subject of a different article [31].

However, the model was largely incapable of satisfactorily reproducing the anisotropy under tension of this same ET || $[0002]$ fiber texture (Figure 2c). Discrepancies corresponded first to the substantial overestimation of the yield stress under tension along ET which corresponded to profuse twinning conditions, and second to the underestimation of the yield stress under tension along ED which corresponded to minimum twinning conditions.

The inability of reproducing the yield stress under ET tension is intriguing. In fact, the onset of plasticity was dominated by both twinning and slip (Figure 2c), as was the case for compression along ED for both ED || $\langle 10\bar{1}0 \rangle$ and ET || $[0002]$ textures. So the model parameters reproducing the anisotropy behaviors under compression for both textures should have been robust enough to predict the yield stress arising for basal and tension twin activities under ET tension.

The underestimation of the yield stress under ED tension is equally intriguing. The onset of plasticity was characterized by a marked activation of both basal $\langle a \rangle$ slip and prismatic $\langle a \rangle$ slip (Figure 2c}). On one hand, the CRSS of prismatic $\langle a \rangle$ slip, i.e. 95 MPa, was identified to be five times greater than that of basal $\langle a \rangle$ slip, i.e. 23 MPa, in order to reproduce the behavior of both the rod texture and basal texture. The CRSSs of pyramidal $\langle c + a \rangle$ slip and tension twinning were 111 MPa and 67 MPa. On the other hand, this very high CRSS value of prismatic $\langle a \rangle$ slip was still insufficiently small to capture the yield stress under ED tension dominated by both $\langle a \rangle$ slips. The impact of underestimating the CRSS of prismatic $\langle a \rangle$ slip under tension can also be sensed under ET tension that is characterized by profuse twinning. In fact, upon reorientation, the twins deformed substantially by prismatic $\langle a \rangle$ slip, so the experimental stress-strain behavior showed a considerably higher hardening rate and a sharper Regime II than the predicted ones.

The phenomenon of concomitant softening of tension twinning and hardening of non-basal slip in polycrystalline magnesium is difficult to understand without considering slip and twinning as competitive deformation mechanisms. One may focus on either why the twinning stress decreases or why the non-basal slip stress increased under tension. The competition between slip and twinning is well known when one thinks of slip and twinning activities under the effect of temperature or strain rates. Twinning is essentially athermal, and it is only needed when pyramidal slip is too hard to activate for accommodating $\langle c \rangle$ axis deformation. When temperature is high enough to lower the CRSS of pyramidal $\langle c + a \rangle$ slip below or closely above that of twinning, twinning tends to disappear. The strain rate has an opposite effect, and there could actually be a ubiquitous combination of strain rate and temperature where twinning is omnipresent.

Although the dependence of twinning and non-basal slip stresses to the loading direction could be understood, the origin of either phenomena is clear. Nonetheless, considering recent simulations reports [15,32–34] on the twinning stress softening induced by a decrease in the grain boundary misorientation, it could be that this softening effect is sensitive to the stress state. In fact, it is well known that Bauschinger effect in cubics was usually correlated to backstress effects [35,36]. Thus, because the GBM effect on the twinning stress can be considered as special case of backstress, it is not surprising to find that this effect can be sensitive to the stress state (tension versus compression).

Figure 3 shows the misorientation distribution of the rod texture and basal texture, respectively. The texture is characterized by a peak in the misorientation angle distribution at the low GBM range (i.e. ≤15°), while the second texture exhibits spiked in the high misorientation range (i.e. ≥70°). Because, basal texture has substantially high fraction of grain boundaries with low misorientations

than the rod texture, according to the above theory by Beyerlein and co-workers on the non-Schmid effects of GBM, twinning should be much softer in the basal texture. The asymmetry observed in this study between the rod texture and basal texture substantiates the accuracy of this theory. To illustrate the effect of GBM misorientation on twinning, non destructive EBSD was performed to compare the growth rates of $\{10\bar{1}2\}$ twins nucleated at low and high misoriented grain boundaries in AM30 Mg.

Modern texture randomization to increase magnesium ductility may have indirectly mitigated twinning not only by reducing the volume fraction of grain with high Schmid factor to twinning, but by further reducing the surface fraction of GBs having low misorientation angles. However, one should note that backstress effects arising from strain incompatibilities at highly misoriented GBs should be more pronounced in weak textures. These backstress effects may restore high activities of tension twinning including detrimental nucleation of contraction twinning.

Conclusions

This paper illustrates that $\{10\bar{1}2\}$ twinning can be strongly promoted in polycrystalline magnesium showing low rotation angles with respect to the *c*-axis. Twinning softening is systematically accompanied by hardening of non-basal slip, which substantiates the competitive nature of slip and twinning as evidenced by the tension-compression asymmetry. This was corroborated by mechanical tests and advanced crystal plasticity models that while able to reliably predict anisotropy even if texture is radically changed, failed to predict the strong asymmetry and resulting anisotropy associated with the grain boundary effects. One may think that grain boundary misorientation is a special case of backstress so the effect of the stress state (tension or compression) may have a similar basis as those models that are invoked for cubic materials.

Acknowledgments

The authors would like to recognize the Center for Advanced Vehicular Systems (CAVS) at Mississippi State University for supporting this work. The authors gratefully acknowledge funding support through the DOE Southern Regional Center for Lightweight Innovative Design award DE-FC26-06NT42755 to carry out a portion of this research work.

This work has benefited from the Lujan Neutron Scattering Center at LANSCE, which is funded by the U.S. Department of Energy, Office of Basic Energy Sciences. Los Alamos National Laboratory is operated by Los Alamos National Security LLC under DOE Contract No. DE-AC52-06NA25396.

References

[1] A. Cottrell, B. Bilby, Philosophical Magazine (Series 7) 42 (1951) 573–581.
[2] R.L. Bell, R. Cahn, Proceedings of the Royal Society of London. Series A, Mathematical and Physical Sciences 239 (1957) 494–521.
[3] G. Bolling, R. Richman, Acta Metallurgica 13 (1965) 709–722.
[4] G. Bolling, R. Richman, Acta Metallurgica 13 (1965) 723–743.
[5] J.P. Hirth, in:, R.E. Reed-Hill, J.P. Hirth, H.C. Rogers (Eds.), Deformation Twinning, Gordon and Breach Science Publishers, 1964, p. 112.
[6] J. Venables, in:, AIME Conference Proceedings, RE Reed-Hill, JP Hirth and HC Rogers (Eds), 1964.
[7] R.E. Reed-Hill, in:, R.E. Reed-Hill (Ed.), The Inhomogeneity of Plastic Deformation, American Society for Metals, Metals Park, OH, 1973, pp. 285–311.
[8] S. Mahajan, D. Williams, International Metallurgical Reviews 18 (1973) 43–61.
[9] A. Sleeswyk, Philosophical Magazine 29 (1974) 407–421.
[10] J.W. Christian, S. Mahajan, Progress in Materials Science 39 (1995) 1–157.
[11] M. Meyers, O. Vöhringer, V. Lubarda, Acta Materialia 49 (2001) 4025–4039.

[12] J. Wang, J. Hirth, C. Tomé, Acta Materialia 57 (2009) 5521–5530.
[13] E. Martin, L. Capolungo, L. Jiang, J.J. Jonas, Acta Materialia 58 (2010) 3970–3983.
[14] L. Capolungo, P. Marshall, R. McCabe, I. Beyerlein, C. Tomé, Acta Materialia 57 (2009) 6047–6056.
[15] I. Beyerlein, C. Tomé, Proceedings of the Royal Society of London. Series A, Mathematical and Physical Sciences 466 (2010) 2517.
[16] S. Mahajan, G. Chin, Acta Metallurgica 21 (1973) 1353–1363.
[17] J.J. Gilman, Transactions of the Metallurgical Society of AIME 206 (1956) 1326–1336.
[18] J.J. Gilman, Acta Metallurgica 3 (1955) 277–288.
[19] J. Holden, Philosophical Magazine 43 (1952) 976–984.
[20] P.L. Pratt, S. Pugh, Journal of the Institute of Metals 80 (1952) 653–658.
[21] R.W. Armstrong, Canadian Metallurgical Quarterly 13 (1974) 187–202.
[22] H.R. Wenk, L. Lutterotti, S. Vogel, Nuclear Instruments and Methods in Physics Research Section A 515 (2003) 575–588.
[23] H.R. Wenk, L. Lutterotti, S.C. Vogel, Powder Diffraction 25 (2010) 283–296.
[24] R. Hielscher, H. Schaeben, Journal of Applied Crystallography 41 (2008) 1024–1037.
[25] I. Beyerlein, C. Tomé, International Journal of Plasticity 24 (2008) 867–895.
[26] H. Mecking, U. Kocks, Acta Metallurgica 29 (1981) 1865–1875.
[27] U. Kocks, H. Mecking, Progress in Materials Science 48 (2003) 171.
[28] R. Lebensohn, C. Tomé, Acta Metallurgica Et Materialia 41 (1993) 2611–2624.
[29] A.L. Oppedal, H. El Kadiri, C.N. Tomé, G.C. Kaschner, S.C. Vogel, J.C. Baird, M.F. Horstemeyer, International Journal of Plasticity 31 (2012) 41–61.
[30] H. El Kadiri, A. Oppedal, Journal of the Mechanics and Physics of Solids 58 (2010) 613–624.
[31] A.L. Oppedal, H.E. Kadiri, C.N. Tomé, J.C. Baird, S.C. Vogel, M.F. Horstemeyer, (2012).
[32] I. Beyerlein, L. Capolungo, P. Marshall, R. McCabe, C. Tomé, Philosophical Magazine 90 (2010) 2161–2190.
[33] I. Beyerlein, R. McCabe, C. Tomé, Journal of the Mechanics and Physics of Solids 59 (2011) 988–1003.
[34] J. Wang, I. Beyerlein, C. Tomé, Scripta Materialia 63 (2010) 741–746.
[35] C. Frederick, P. Armstrong, Materials at High Temperatures 24 (2007) 1–26.
[36] B. Chun, J. Jinn, J.K. Lee, International Journal of Plasticity 18 (2002) 571–595.

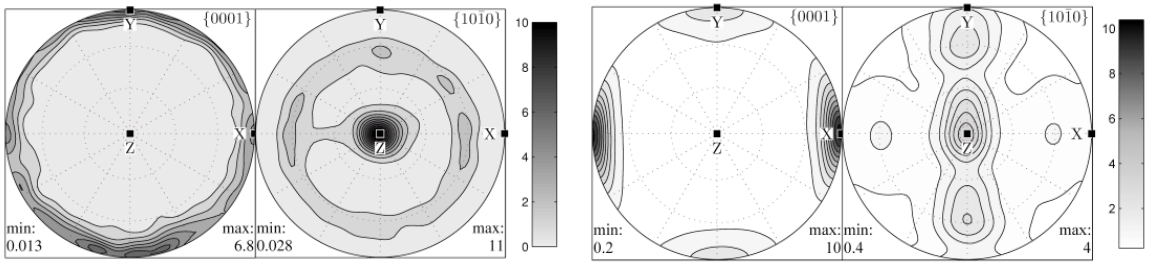

a) b)

Figure 1. Recalculated [0001] and <10-10> pole figures obtained by neutron diffraction data revealing for an AM30 magnesium alloy (a) an axisymmetric rod texture, and (b) a strong [0001] fiber with a perpendicular secondary weak spot. For the axisymmetric texture, X and Y correspond to radial directions (ET) normal to the extrusion direction (ED) Z, while for the second [0001] fiber, Z is the extrusion direction (ED), Y is the normal direction (EN) to the sheet, and X is a transverse direction in the plane of the sheet (ET). Thus, axisymmetric extrusion and plane-strain extrusion led to a main ED || <10-10> and ET || <0002> components, respectively.

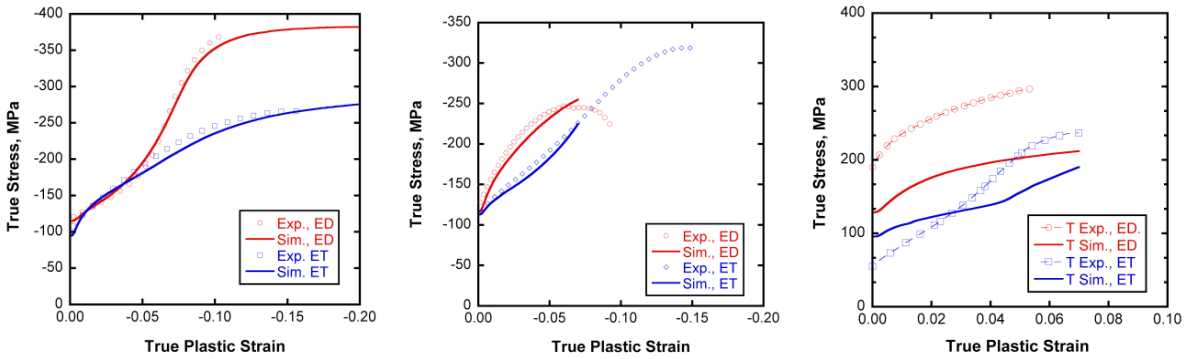

a) b) c)

Figure 2. Results of experimental and simulation tests including the (a) stress-strain curves for compression along ED and ET of the rod texture corresponding to the behavior that was used to identify the crystal plasticity parameters for a best fit, (b) stress-strain curves for compression along ED and ET of the ET || [0001] fiber where the simulated curves were generated using the same crystal plasticity parameters identified by fitting the behavior of the rod texture in compression, (c) stress-strain curves for tension along ED and ET of the ET || [0001] fiber where the simulated curves were generated using the same crystal plasticity parameters identified by fitting the behavior of the rod texture in compression.

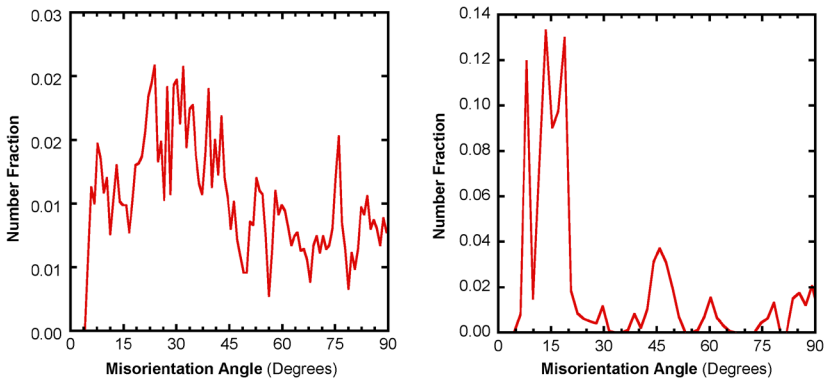

a) b)

Figure 3. Misorientation distribution charts for (a) the ED || <10-10> fiber, and (b) ET || <0002> fiber. The first fiber contains a significant fraction of highly misoriented grain boundaries (>15°) while the second one has most grain boundaries with low misorientation angles (<15°).